Scientific Journal of Impact Factor (SJIF): 4.72
e-ISSN (O): 2348-4470
p-ISSN (P): 2348-6406

International Journal of Advance Engineering and Research Development

Volume 4, Issue 9, September -2017

Investigation of Site Selection & Designing of Dual Rotor Horizontal Axis Wind Turbine System for small scale site at RGPV Hill Top.

Anurag Gour, Mukesh Pandey, VK Sethi

[1*]*Assistant Professor, School of Energy and Environmental Management, UTD, RGPV Bhopal, MP, INDIA*
[2]*Professor, Dean & Head, School of Energy and Environmental Management, UTD, RGPV Bhopal, MP, INDIA*
[3] Former Director, *UIT, RGPV Bhopal, MP, INDIA*a

ABSTRACT:- *Renewable energy resources like wind energy is one of the most significant and rapidly developing renewable energy on this planet. For the next leap in the wind energy conversion technologies, we are under adherence not only to face with the environment challenges but also to conserve natural ecosystem. The majority of wind turbines currently in operation have the conventional concept design; single rotor wind turbine and electric generator. Recently, Dual-Rotor wind turbine (DRWT) has been introduced to the market. This review paper is concerned on investigation of site selection, design, development and fabrication of Dual Rotor wind turbine system on the basis of wind flow characteristic at RGPV Hill-top. The purpose of this article is to addressing the general aspects of this area of knowledge and contextualizing it to perform an investigation on wind flow characteristics and to determine the Annual Energy Production (AEP) of existing wind turbines installed at the same site. In this work, the recorded time series wind data fetched by the NRG Symphonie Data logger wind mast installed at Energy Park, RGPV campus. This review article is for presentation on research on the aerodynamics of wind turbine blade using Computational Fluid Dynamics (CFD) and Design of Dual rotor Gearbox technological system on CATIA software. A counter-rotating wind turbine having two rotors rotating in opposite directions on the same axis is proposed to improve the aerodynamic performance of a wind turbine wind turbine blade is most important component to produce electricity from wind. An enhanced understanding of how small wind turbines interact with wind turn out to be essential. The design unit is composed of the tandem wind rotors, whose front and rear diameters are 1.0 meter and 3.0 meter respectively. Wind turbine blades are subjected to different types of forces. Currently research has concentrated to improving the aerodynamics performances of wind turbine blade through wind tunnel testing and theoretical studies. However wind turbine simulation through computational Fluid Dynamics (CFD) software offers easy solution to aerodynamics blade analysis problem. The challenges of optimisation within other aerodynamics fields were identified.*

Keywords: *-Wind Energy Aerodynamics, WAsP, Wind Rose, OWC, Wind Atlas, AEP, Ansys Fluent-CFD, Computational Flow Optimization, Gearbox, CATIA.*

1. INTRODUCTION

Recently, the growing public awareness of the environmental concerns, limited energy supply and uncertain energy prices has spearheaded in promotion of wind power. Wind energy has experienced a remarkable expansion in the past year. It presents attractive opportunities to a wide range of promoters including investors and entrepreneurs. The majority of wind turbines currently in operation have the conventional concept design. That is a single-rotor wind turbine system which is connected through transmission system (gearbox) to a generator. Recently, the research on dual-rotor wind turbine is undertaking by individuals researcher and manufacturer introduced to the concept to the market.

In this review paper we operated on WAsP software to give accurate climatological prediction over low smooth hills of RGPV Bhopal. This software uses the Reynolds-Average Navier-Stokes equation to create a linear model, Wind Atlas, to solve wind flow equations. Computational Flow Optimization (CFO) technique is used for optimization of aerofoil design using CFD method. The design parameters that are involved in dual-rotating wind turbine are more descriptive than that of a single rotor wind turbine because of the complex phenomenon arising from the aerodynamic interaction between its two rotors. It has been proven that the steady state performance of the dual-rotor wind turbine system for extracting energy is better than the Single-Rotor wind turbine system (SRWT). The Dual-rotor wind turbine has two rotors, rotating in clockwise and/or counter clockwise, depending upon gear transmission system employed. It has been proposed, on the basis of the theory that a configuration of two rotors having the same swept area on the same axis has higher maximum power coefficient than a conventional configuration of a wind turbine having a single rotor. [13]

The proposed gearbox system composed of both compound and planetary gear train. The rotor rotates at 60-70 RPM in case of large capacity wind turbines and 100-300 RPM in small wind turbines. The large wind turbine requires efficient gearboxes to convert small rotational speed of 70 RPM to the high rotational speed of 1600-1800 RPM. The rated speed for the wind turbine is taken 10m/s, Local cut in speed as 2.5m/s and cut out speed 25m/s.

2. MAP

The map for the selected area is downloaded from Shuttle Radar Topography Mission (SRTM) data, which offers maps of high resolution. SRTM elevation data has now been released for the entire terrestrial surface.

2.1 Height Contours

In WAsP simulations the landscape complexity is described by height contours. These height contours lines are generated by importing Digital Elevation Model (DEM) files of RGPV and surrounding to Global Mapper software, which is to be done by the help of SRTM data.

These files are then exported as a shape file (.shp) which is presented in (Figs. 2 and 3) shows the Roughness lines and contour lines of the area exported using shape files. The height contour lines are essential since change in height influences the turbulence and consequently the wind profile.

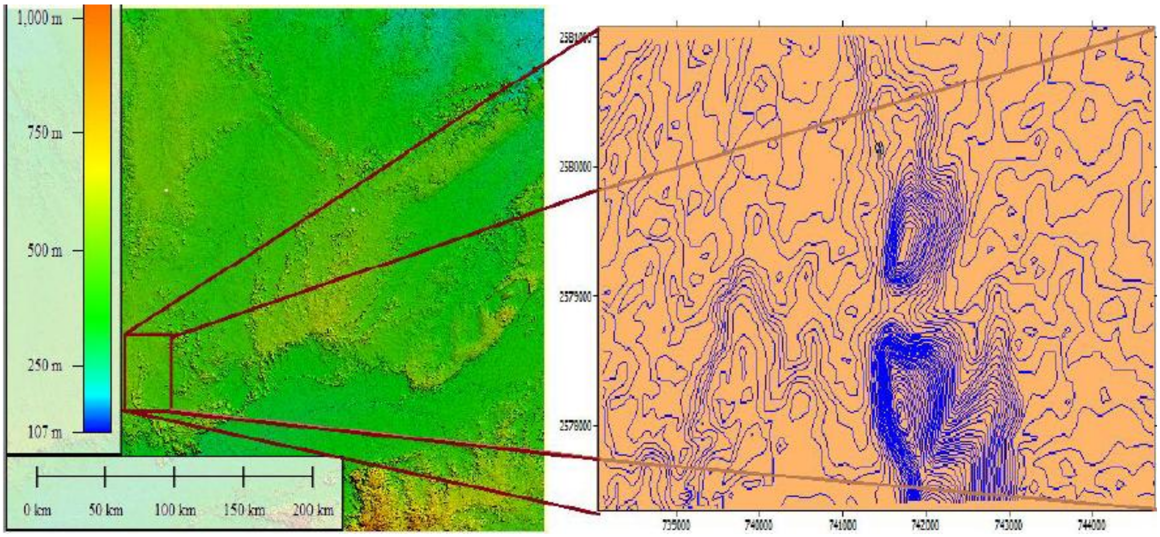

Fig. 1 SRTM map of RGPV energy park, Bhopal (India)

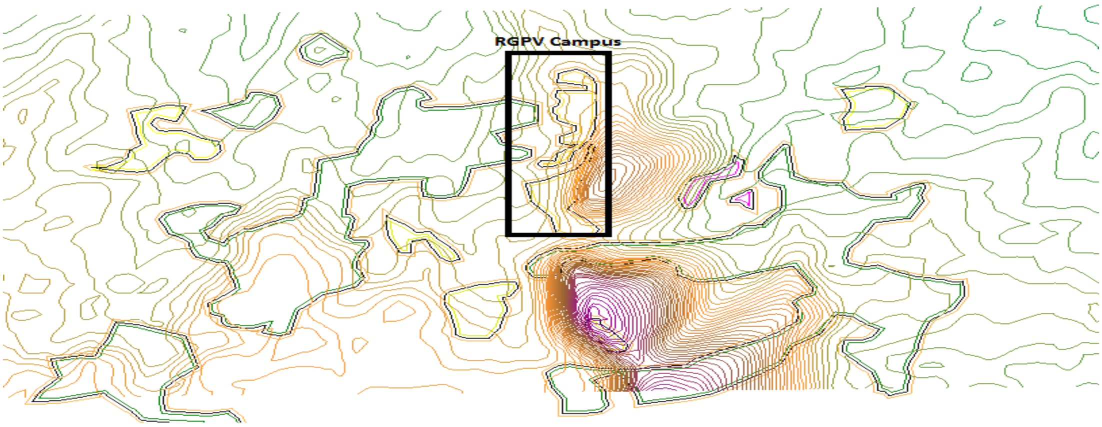

Fig. 2 Combined map with Roughness lines and Contour lines

2.2 Roughness Class

The roughness of a particular surface area is determined by the size and distribution of the roughness elements it contains for land surfaces these are typically vegetation, built-up areas and the soil surface.

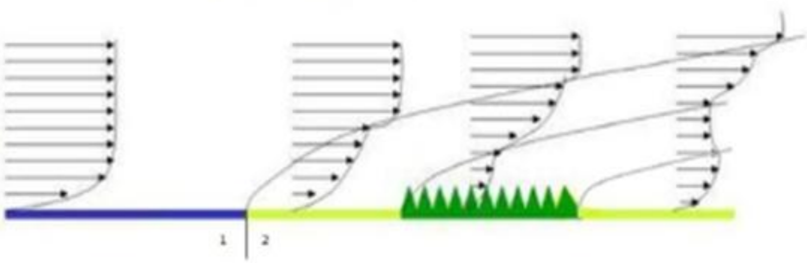

Fig. 3 Effects of change in roughness on boundary layer

Wind profile is dependent on the roughness of the surface. Turbulence increases when there is a change in roughness. This change the height of the internal boundary layer as demonstrated in (Fig. 4). Roughness is classified in different categories and is given certain length. This is presented in the Table 1.

Table 1 Roughness type and length (roughness length is 1/30th of the actual length of the element)

Area Type	Roughness Length (m)
Water areas e.g. lakes, ocean etc.	0.002
Farmland with open-appearance / buildings / trees	0.03
Farmland with closed appearance	0.10
Suburbs, shelter belts, trees & bushes	0.40
Tall forest	1.50

2.3 Convert to .map

Both height contours and roughness lines are converted into .map format. This is done only because WAsP requires this format type in their simulations [1]

3. WIND DATA

The wind data was recorded by the NRG Symphonie data logger which is installed at geographical location of East 077' 21.668 and North 23' 18.720 and the elevation of mast base is 591 meters. At the wind measurement mast, a 3 cup type anemometer with measuring height of 20 meter along with two wind vanes at the heights of 20 and 38 meters is assembled as shown in (Fig. 5). It also provides the measurements for relative humidity, atmospheric pressure, temperature and rain gauge.

Fig. 4 Wind masts at energy park, RGPV

Site Information:

Project: New Project

Location:

Elevation: 591

Sensor Information:

1 NRG #40C Anem m/s
2 NRG #40C Anem m/s
3 NRG #40C Anem m/s
4 No SCM Installed
5 No SCM Installed
6 No SCM Installed
7 NRG 200P Vane deg
8 NRG 200P Vane deg
9 NRG 110S Temp C
10 NRG BP20 Baro mb
11 No SCM Installed
12 iPack Voltmeter
13 NRG #40C Anem m/s
14 NRG #40C Anem m/s
15 NRG #40C Anem m/s

9/1/2013 to 8/31/2014

Summary Report

SITE 4444

New Site

Channel	1	2	3				7	8	9	10		12	13	14	15
Height	40 m	40 m	20 m	-----	-----	-----	38 m	20 m	6 m	3 m	-----	m	0	0	0
Units	m/s	m/s	m/s	-----	-----	-----	deg	deg	C	mb	-----	Volt	m/s	m/s	m/s
Intervals with Valid Data	51924	51924	51924				51924	51924	51924	51924		51924	51924	51924	51924
Average Filtered Data	3.86	3.88	2.63				340.93	323.44	25.58	948.41		13.47	0.4	0.4	0.4
Average for All Data	3.86	3.88	2.63				340.93	323.44	25.58	948.41		13.47	0.4	0.4	0.4
Min Interval Average	0.3	0.4	0.4						8	933.4		13.1	0.4	0.4	0.4
Date of Min Interval	9/9/2013	9/9/2013	9/1/2013						1/12/2014	7/23/2014		4/11/2014	9/1/2013	9/1/2013	9/1/2013
Time of Min Interval	12:00:00 AM	12:00:00 AM	7:20:00 PM						6:50:00 AM	3:10:00 AM		6:30:00 AM	12:00:00 AM	12:00:00 AM	12:00:00 AM
Max Interval Average	17.5	17.5	13.4						45.1	961.1		14.3	0.4	0.4	0.4
Date of Max Interval	4/20/2014	4/20/2014	4/20/2014						6/6/2014	1/19/2014		2/17/2014	9/1/2013	9/1/2013	9/1/2013
Time of Max Interval	9:30:00 PM	9:30:00 PM	9:30:00 PM						2:50:00 PM	10:50:00 AM		8:10:00 AM	12:00:00 AM	12:00:00 AM	12:00:00 AM
Average Interval SD	0.77	0.78	0.79				11.42	17.79	0.11	0.15		0	0	0	0
Min Sample	0.3	0.4	0.4						7.9	933.4		13	0.4	0.4	0.4
Date of Min Sample	9/1/2013	9/1/2013	9/1/2013						1/12/2014	7/23/2014		6/12/2014	9/1/2013	9/1/2013	9/1/2013
Time of Min Sample	2:50:00 PM	10:40:00 PM	12:00:00 AM						6:50:00 AM	2:40:00 AM		6:00:00 AM	12:00:00 AM	12:00:00 AM	12:00:00 AM
Max Sample	38.2	36.7	33.7						45.5	961.5		14.7	0.4	0.4	0.4
Date of Max Sample	4/17/2014	4/17/2014	4/17/2014						6/6/2014	1/19/2014		1/7/2014	9/1/2013	9/1/2013	9/1/2013
Time of Max Sample	6:20:00 PM	6:20:00 PM	6:20:00 PM						2:40:00 PM	10:20:00 AM		9:20:00 AM	12:00:00 AM	12:00:00 AM	12:00:00 AM
Average Interval TI	0.23	0.23	0.34										0	0	0
Wind Speed Direction							W	W							

Generated Saturday, September 20, 2014

NRG Systems SDR Version 7.03

Fig. 5 Device Report

A data logger was connected with all sensors on the mast to collect data in time series, which has a fixed averaging interval of 10 minutes. For each of the 12 channels averages, standard deviations, minimum values and maximum values are calculated from continuous 2 second data samples. Data intervals are calculated every 10 minutes, time stamped with the starting time of each interval and written to the Multi-Media Card at the top of each hour. (Fig. 6) shows the Device Report of NRG system.

4. WAsP

WAsP is software which calculates energy output based on a linear flow model and is reliant on input wind data. This tool is used to estimate and optimize wind farm energy production generate wind resource maps. This software uses the Reynolds-Average Navier-Stokes equation to create a linear model, Wind Atlas, to solve wind flow equations. This Model requires wind data, height contour lines, and Roughness map of the area to calculate energy production of a wind turbine [Karl, J.N., 2010, "Estimation of wind energy production in relation to orographic complexity".].

WAsP can be used for various purposes such as:

- Estimating and optimizing wind farm production and efficiency,
- Mapping of wind resources and
- Digitalizing information on maps, such as height contours.

5. OBSERVED WIND CLIMATE

In the observed wind climate file, the frequencies of occurrence of the wind in a number of sectors (the wind rose) and wind speed bins is represented. This also contains the height of observation above ground level and the geographical coordinates (latitude and longitude) of the wind mast.

Table 2 Sector wise parameters at 20 Meter

Sectors	A	K	U	P	F
0	2.9	1.57	2.58	27	4.4
30	2.4	2.13	2.09	10	7.8
60	2	2.05	1.77	6	13
90	2.2	2.22	1.96	8	12.2
120	2.1	2.17	1.84	7	6.9
150	2	2.12	1.80	6	3.4
180	2.4	1.79	2.12	13	2.2
210	3.1	2.10	2.73	23	6.1
240	3.3	2.08	2.91	28	9.1
270	4.1	2.57	3.67	47	17.7
300	3.8	2.75	3.40	36	11.8
330	3.2	1.82	2.84	30	5.6
All	2.9	1.81	2.59	23	100

The values of Weibull Parameters (A, k), mean wind speed (U), mean power density (P) and frequency of all 12 sector (0° to 359°) is calculated from WAsP OWC Wizard and recorded in Table 2 for 20 meter height respectively.

Table 3 Measured and Emergent Mean Wind Speed and Power Density

	Mean Wind Speed	Mean Power Density
Measured at 20 m	2.45 m/s	19 W/m^2
Weibull-fit at 20 m	2.62 m/s	23 W/m^2
Discrepancy at 20 m	1.2 %	2.0 %

The measured discrepancy and the Weibull fitted values of mean wind speed and mean power density for 20 meter height is shown in Table 3.

6. WIND ROSE AND WEIBULL HISTOGRAM

A wind rose is a diagram that depicts the distribution of wind direction and speed at a location over a period of time on the basis of meteorological observations of wind speeds and wind directions. The length of each spoke on a wind rose indicates how often the wind comes from this direction [http://www.crh.noaa.gov/grr/aviation/mkg/]. The meaning of longer spokes is the wind comes from this direction more often. A Wind rose is made from dividing the compass into 12 sectors equally, each for 30 degrees of the horizon. (A wind rose can also be drawn for 8 or 16 sectors, but 12 sectors is standard set by the European Wind Atlas) [Mortensen, N.G. Heathfield, D.N. Rathmann, O. and Morten, N., 2013, "Wind Atlas Analysis and Application Program: WAsP 11 Help Facility.].

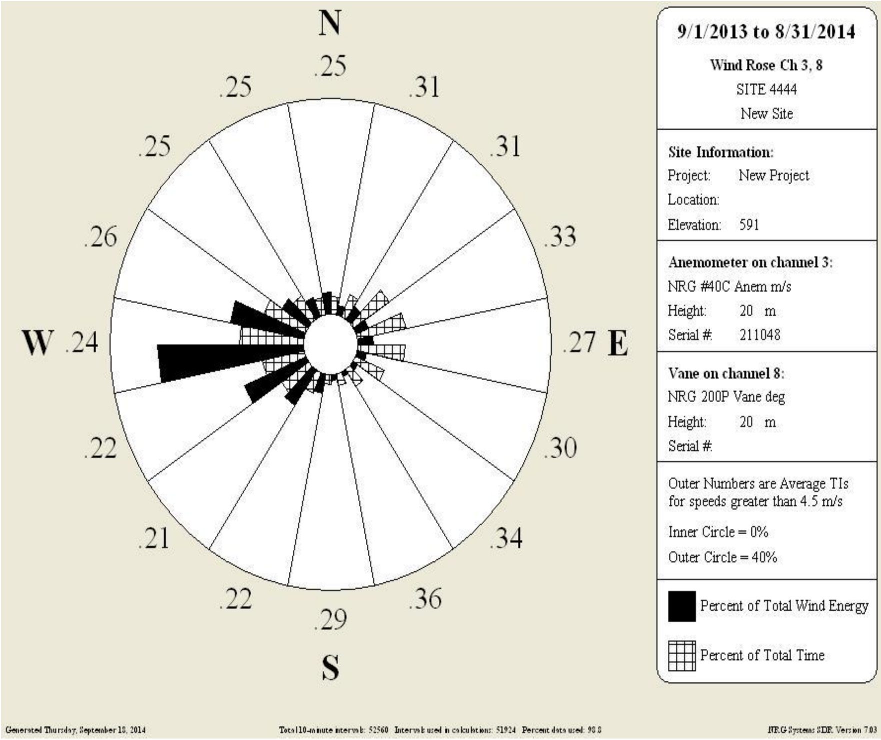

Fig.6 Wind rose generated by Symphonie software

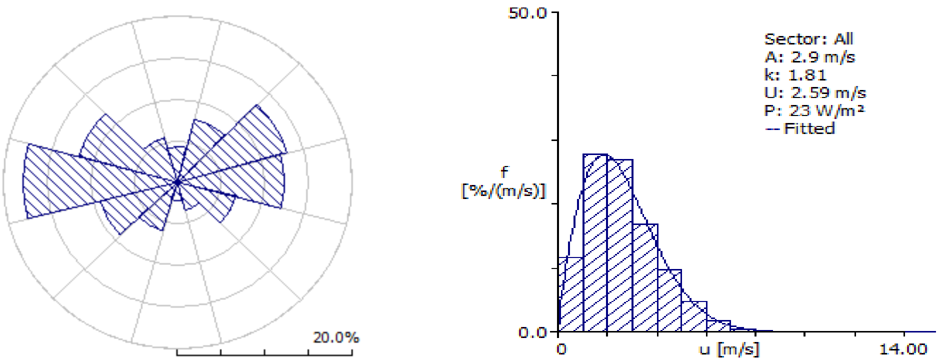

Fig. 7 Wind Rose and Spectrum of Energy Park Mast, RGPV

In (Figs. 7 and 8) the wind rose, wind speed histograms and Weibull approximation is shown for 20 meter meteorological height respectively.

7. GENERALIZED WIND CLIMATE

The observed wind data is converted into a generalized wind climate (GWC). The wind observations have been cleaned in terms of site specific conditions such as: surface roughness, shelter (buildings etc.) and orography. This information was then converted into a map format. When the data has been converted into standard conditions, for four standard roughnesses, five standard heights above ground and 12 azimuth sectors, it can then create a general wind atlas. When the wind atlas data has been generated, WAsP can estimate the wind climate at any particular point by performing the inverse calculation as is used to generate the wind atlas [Sveinbjornsson, S., 2013, "Analysis of WAsP (Wind Atlas Analysis and Application Program) in Complex topographical Conditions using measured production from a large scale wind farm].

The wind atlas containing 5 standard heights and 5 standard roughness classes are shown in the Table 4 for 20 meter height respectively.

Table 4
Wind atlas at 20 meter

Height	Parameter	0.00 m	0.03 m	0.10 m	0.40 m	1.50 m
10.0 m	Weibull A [m/s] Weibull k Mean speed [m/s] Power density [W/m²]	3.4 1.87 2.99 34	2.5 1.73 2.19 15	2.1 1.73 1.91 10	1.7 1.72 1.51 5	1.1 1.65 1.00 1
15.0 m	Weibull A [m/s] Weibull k Mean speed [m/s] Power density [W/m²]	3.5 1.88 3.11 38	2.7 1.76 2.37 18	2.4 1.76 2.10 12	1.9 1.75 1.72 7	1.4 1.67 1.23 3
20.0 m	Weibull A [m/s] Weibull k Mean speed [m/s] Power density [W/m²]	3.6 1.89 3.20 41	2.8 1.80 2.51 21	2.5 1.79 2.24 15	2.1 1.78 1.87 9	1.6 1.69 1.39 4
25.0 m	Weibull A [m/s] Weibull k Mean speed [m/s] Power density [W/m²]	3.7 1.90 3.27 43	3.0 1.83 2.62 23	2.7 1.82 2.36 17	2.2 1.80 1.99 10	1.7 1.71 1.52 5
30.0 m	Weibull A [m/s] Weibull k Mean speed [m/s] Power density [W/m²]	3.8 1.92 3.33 45	3.1 1.86 2.72 25	2.8 1.85 2.46 19	2.4 1.83 2.09 12	1.8 1.73 1.63 6

8. ESTIMATION OF POWER PRODUCTION OF TURBINE

The frequency of occurrence of a given wind speed is determine by the probability density function or distribution function. Estimating the relevant probability density function or Weibull distribution is the key purpose of the wind atlas methodology.
Hence, to calculate the power production of a wind turbine or wind farm, we need the predicted wind climate for the site and the following turbine characteristics.

8.1 The wind turbine hub height [m]
8.2 The power curve [ms^{-1} and kW]
8.3 The thrust coefficient curve

8.1 The Wind Turbine Hub Height

In general, the hub height is the nominal hub height given by the wind turbine manufacturer. This is the height provided in the wind turbine data files. However, in certain situations the precise meaning of height above the ground is not evident.

8.2 The Power Curve

Once the power curve $P(u)$ is measured for a wind turbine, the mean power production can be estimated provided the probability density function of the wind speed at hub height is determined by a siting procedure.

$$P = \int_0^{\infty} Pr(u)P(u)d(u)$$

The power production by a wind turbine varies with the wind that strikes the rotor. The power produced as function of the wind speed at hub height is called the *power curve*. The (Fig. 9) shows a power curve of 10 kW Machinocraft wind turbine generator.

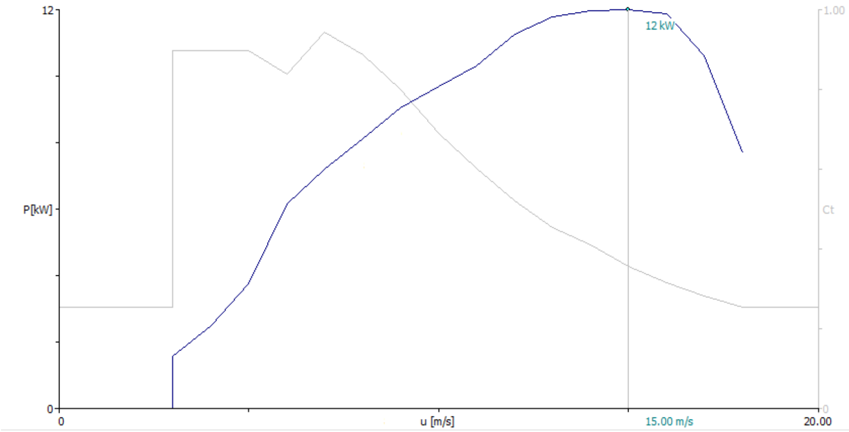

Fig. 8 Power curve of 10 kW Machinocraft wind turbine generator

When the wind speed is less than the *cut-in* wind speed, the turbine will not be able to produce power. When the wind speed exceeds the cut-in speed, the power output $P(u)$ increases with increasing wind speed to a maximum value, the *rated power*; thereafter the output is almost constant. At wind speeds higher than the *cut-out* speed the wind turbine is stopped to prevent structural failures.

8.3 Thrust Coefficient Curve

The thrust coefficient must be specified in order to calculate wind farm wake effects and wind farm efficiency. WAsP can estimate the wake losses for each turbine in a farm by giving the power and thrust coefficient curves of the wind turbine and the wind farm layout and thereby the net annual energy production (AEP) of each wind turbine and of the entire farm.

9. RESOURCE GRID MAPS

Resource grids provide a rectangular set of points for which summary predicted wind climate data are calculated. The points are regularly spaced and are arranged into rows and columns, which shows a pattern of wind climate or wind resources for an area.
Each point in the grid is like a simpler version of a normal turbine site. All the points have the same height a.g.l. If a wind turbine generator is associated with the grid, then that specification is used for all of the points in the grid. The resource grid always shows the gross annual energy production without taking into account the occurrence of any turbines in the area (hierarchy). Likewise, the wind speeds and power densities are 'unobstructed', i.e. no wake effects from any turbines affect these values [4].

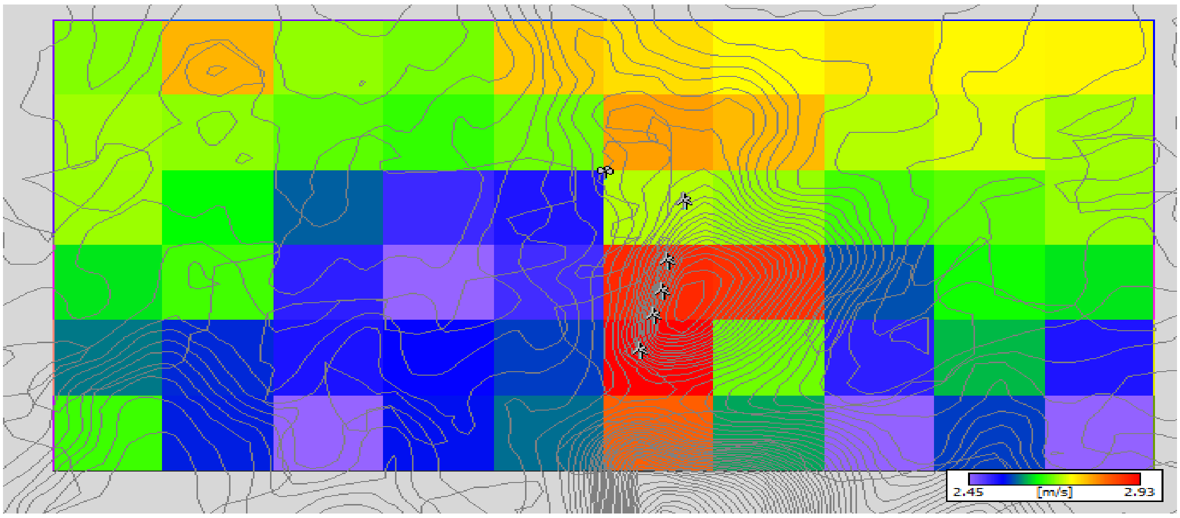

Fig. 9(a) Mean wind speed of resource grid at 20m

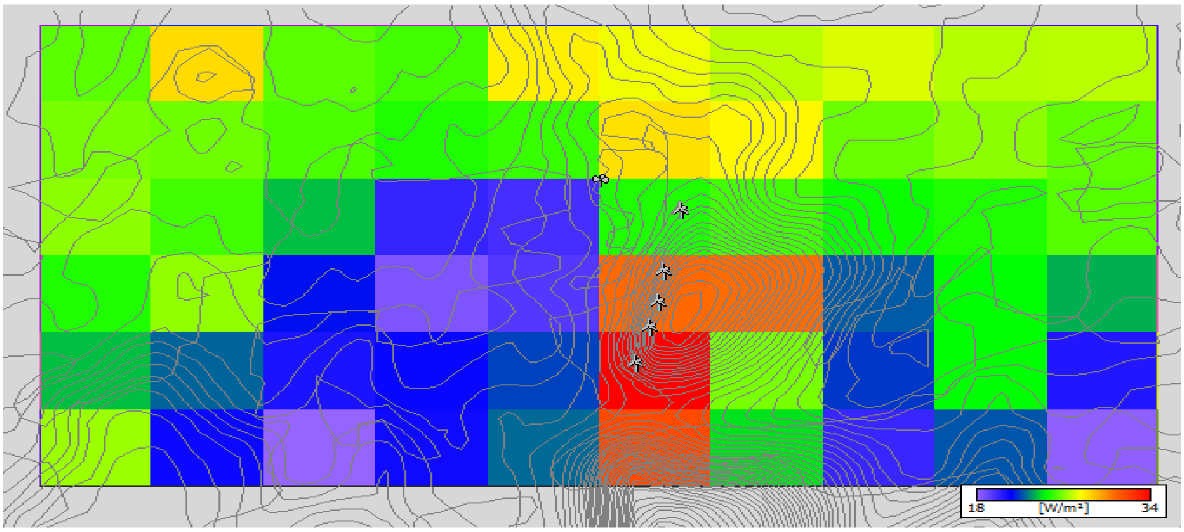

Fig. 9(b) Power density of resource grid at 20m

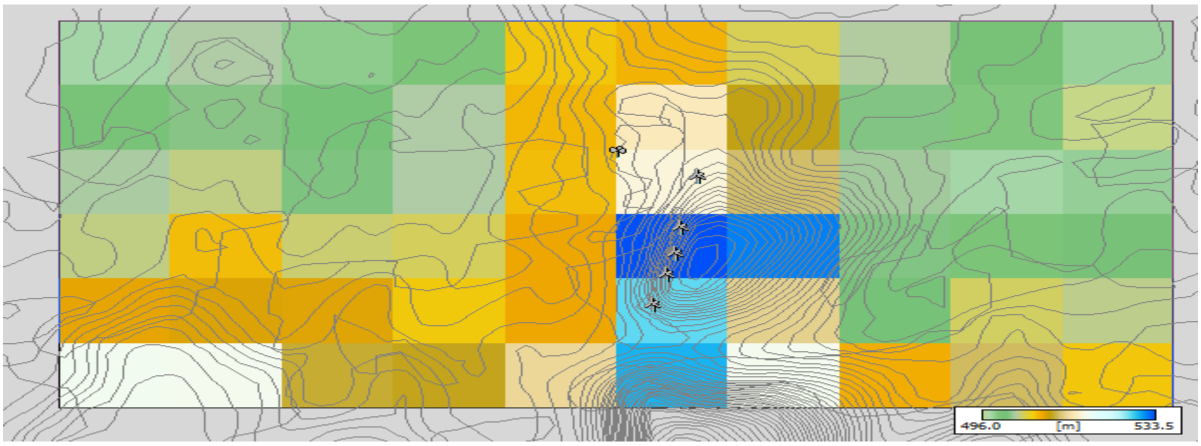

Fig. 9(c) Elevation Profile of Resource Grid

Fig. 9 Resource Grid Maps for RGPV Hill Top

For each point in the grid, WAsP calculates the following data which can be displayed in the resource grid, as shown in (Fig 9).

- The elevation
- The mean wind speed
- The mean power density

10. AERODYNAMICS AND BLADE DESIGN THEORY

Aerodynamic performance is fundamental for efficient rotor design. Aerodynamic lift is the force responsible for the power yield generated by the turbine and it is therefore essential to maximise this force using appropriate design [35]. A resistant drag force which opposes the motion of the blade is also generated by friction which must be minimised. It is then apparent that an aerofoil section with a high lift to drag ratio, typically greater than 30, be chosen for rotor blade Coefficient of lift, Lift to Drag Ratio, Coefficient of drag.A wind turbine exist several main parts, i.e. the rotor, generator, gearbox, yawing system, control system and so on. The rotor is driven by the wind and rotates at predefined wind speed, so that the generator can produce electric energy output under the regulation of the control system. To extract the maximum kinetic energy from wind, researcher put much effort on the design of effective blade geometry. This research aims to evaluate the aerodynamics performance of small horizontal-axis wind turbine blades through two and three dimensional computational fluid dynamics (CFD) analysis.

10.1 Computational Fluid Dynamics (CFD) based approach for Horizontal Axis wind turbine.

The success of any optimisation design is dependent on the clear definition of the design objective as well as the limitations on the solution space. Definition of the solution space is dependent on the extent of freedom of the design

variables. Optimisation methodology is widely applied due to the increasing of multi-variable problems within engineering.
This method is extremely lengthy due to the iterative nature of CFD software and optimisation methods. Generally, the design geometry as well as the mesh of the flow field is optimised. This leads to a vast increase in design variables for optimisation. Furthermore, the automation of CFD within an optimisation program is an intricate task.
Vanderplaats, 1979 describing the simple means of airfoil geometry a main focus of his research was to improve the efficiency of the automated design capability. The efficiency was measured by the number of times the aerodynamics program is called for a complete analysis of the airfoil geometry. Firstly, polynomials were used to describe the airfoil's upper and lower surfaces. The polynomial coefficients were the design variables. Secondly, the airfoil geometry was described in terms of generic shape functions or basis vectors. The generic shape functions were blended to produce the resultant airfoil. The blending fractions became the design variables. This second method of airfoil representation resulted in an increase in optimisation efficiency by a factor of two. Furthermore, this method proved to be robust and versatile to different optimisation techniques [14].
Selig and Maughmer (1992) laid out a generalised multipoint inverse airfoil design where a velocity distribution yielding the desired boundary-layer development is designed using inverse boundary-layer methods. The velocity distribution is changed according to experience and feedback from successive analyses .The airfoil design thus relies on the intuition of the programmer and does not use optimisation methods [6].
Drela (1998) described the fractional arc lengths of the airfoil shape. The airfoil design thus relies on the intuition of the programmer and does not use optimisation methods. In his research on the pros and cons of airfoil optimisation, the airfoil shape was then optimised to fulfil a minimum drag requirement [5].
The challenges of optimisation within other aerodynamics fields were researched. Optimisation methods have been applied to airfoil design using CFD. This is commonly known as computational flow optimisation (CFO). This method is extremely lengthy due to the iterative nature of CFD software and optimisation methods. Generally, the design geometry as well as the mesh of the flow field is optimised. This leads to a vast increase in design variables for optimisation. Furthermore, the automation of CFD within an optimisation program is an intricate task. In general, better CFD results are obtained when mesh refinements are tailored to the design geometry. However, to ensure repeatability in the optimisation iteration, the mesh has to be the same for each design [4].

The results yielded physically unrealisable airfoils with the occurrence of bumps on the surface of the airfoil. The optimizer created these bumps to compensate for the separation bubbles which occur along the surface. These small-scale irregularities had almost no aerodynamic penalty with the result that they were invisible to the optimiser. Furthermore, the airfoil shape had many design parameters or degrees of freedom. Thus, the method laid out in the research paper was of high computational cost. These researches brought particular attention to the importance of limitations on design variables. In effect, an optimizer does not experience of a human programmer and will thus not recognise infeasible solutions.

In CFD software, wind turbines are simulated under the turbulent flows. Normally, the method of turbulent numerical simulation consists of two main parts, which are Direct Numerical Simulation(DNS) and Indirect Numerical Simulation(INS). Although DNS has a precise calculated result,but the whole range of spatial andtemporal scalesof the turbulence mustberesolvedwhich requires a very small time step size, hence this is not suitable for CFD simulation. There are three different types of simulated methods under the Indirect Numerical Simulation which are large eddy simulation (LES), Reynolds-averaged Navier-Stokes (RANS) and detached eddy simulation (DES).

LES has more attraction to rotor wake analysts, but is still prohibited to deal with the near surface regions due to its huge computational overhead. Therefore, a combined approach, detached eddy simulation (DES), in which RANS and LES are adopted in the near-surface and far-surface, respectively, has been proved to obtain good solution. [3]
DNS, which directly solves full Navier-Stokes equation sand needs to catch all relevant scales of turbulence with ultrafine computational grid, is currently impossible to be applied in full wind turbine own field.

Inorder to simulate turbulent flows, theoretically, the computational domain should be big enough to contain the biggest eddy. Meanwhile, the mesh should be small enough tofindout the smallest eddy. But the current grid was too coarse to catch the smalled dies.Hence large eddy simulation (LES) is a technique which filters small eddies while conserving large energy eddies. This method requires a more refined mesht han RANS model, but a far coarser mesh than DNS solutions. The RANS equation is not closed due to the presence of stress term, so it require a turbulence model to produce a closed system of solvable equation. The turbulence model contains one and two equations model. The famous one equation "Spalart-Allamaras" model and two equations "standard k-ε" models are widely used in most CFD softwares. The transport equation of Spalart-Allamaras can be described as:

$$\frac{\partial \bar{\upsilon}}{\partial t} + \tilde{u}\frac{\partial \bar{\upsilon}}{\partial xj} = Cb1\hat{S}\tilde{\upsilon} + \frac{1}{\sigma}\left\{\frac{\partial}{\partial xj}(v + \tilde{\upsilon})\frac{\partial \bar{\upsilon}}{\partial xj} + Cb2\ \frac{\partial \bar{\upsilon}}{\partial xj}\frac{\partial \bar{\upsilon}}{\partial xj}\right\} - Cw_1 f1\left(\frac{\upsilon}{d}\right)^2$$

Where $\tilde{\upsilon}$ *is* the turbulent kinematic viscosity, $Cb1$ is the production of turbulent viscosity and $Cb2$ is the destruction of turbulent viscosity. [7]

11. BLADE MODELLING

In this paper design and modelling of the Dual Rotor Horizontal Axis Wind Turbine (DRWT) blade, and analysed of the both Front and Rear Rotor with Naca Air profile for different Angle of Attack and wind speed. Wind turbine generator output is 1.5 kW, which is gain through the combination of both rotors. Air density is 1.225 kg/m^3 which are constant. Power coefficient of the wind turbine is 0.30 and design wind speed is 10 m/s. In table 1, shows the Dual Rotor Wind Turbine modelling.

TABLE 1: Modelling Data
There are many CFD softwares used in engineering, such as PHOENICS, STAR-CD, and ANSYS FLUENT/CFX and so on. Three main processors are the same which are Pre-Processor, solver and Post Processor.
Setting of the governing equation is the precondition of CFD modelling, mass and momentum and energy conservation equation are three basic governing equations. After that, Boundary conditions are decided as different flow conditions and a mesh is created. The purpose of meshing model is discretised equation and boundary conditions into a single grid. The basic elements of two-dimensional unstructured grid. Finite volume method (FVM) is used in CFD software such as FLUENT and CFX. Our work used the software ANSYS FLUENT Non License Version Workbench (14.5).

Generate the geometry of the both type of rotor in Design Modeller of the ANSYS FLUENT software as per the Design standard and generate the meshing form in the Design modeller. Create the setup for the solution which is given by the table 2and 3. Run the solution programme at the Angle of Attack *10°* and turbulent viscosity ratio is 10. Run the calculation for the result the Plot the Pressure curve which is shown in the figure 4 and 5.

Design the Front Rotor Blade Airfoil as per the modelling of DRWT 60% power generate through the front rotor and 40% by the rear rotor. Front rotor radius is 0.8m with included the hub and blade radius is 0.70m.As per the Naca airfoil consideration NACA0021 blade is taken for this wind turbine. Design the Rear Rotor Blade Airfoil as per the modelling of DRWT 60% power generate through the front rotor and 40% by the rear rotor. Rear rotor has large size as comparison to front rotor. Rear rotor radius is 1.5m with included the hub and blade radius is 1.4m.As per the Naca airfoil consideration NACA0021 blade is taken for this wind turbine.

Table 2: Geometry of the Front and Rotor Blade Airfoil.

In Ansys fluent, the pressure-based solver is used for the low speed incompressible flow. In the pressure-based solver, pressure and pressure corrections are used for the calculation of pressure field. In CFD software, wind turbines are simulated under the turbulent flows. The turbulence model contains one and two equations model. The one equation "Spalart-Allamaras" model and two equations "standard k-ε" models are widely used in CFD softwares**.**

Table-3: Computational feature of the Front and Rear rotor Airfoil on CFD

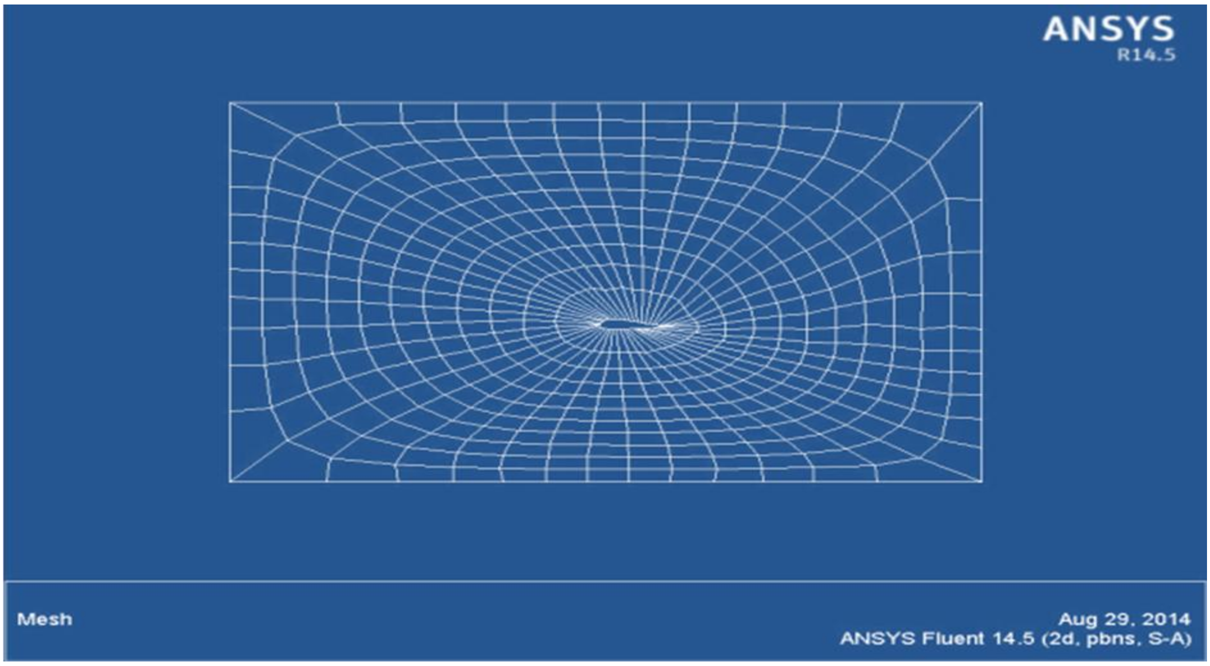

Figure 11: Meshing geometry of the Front rotor

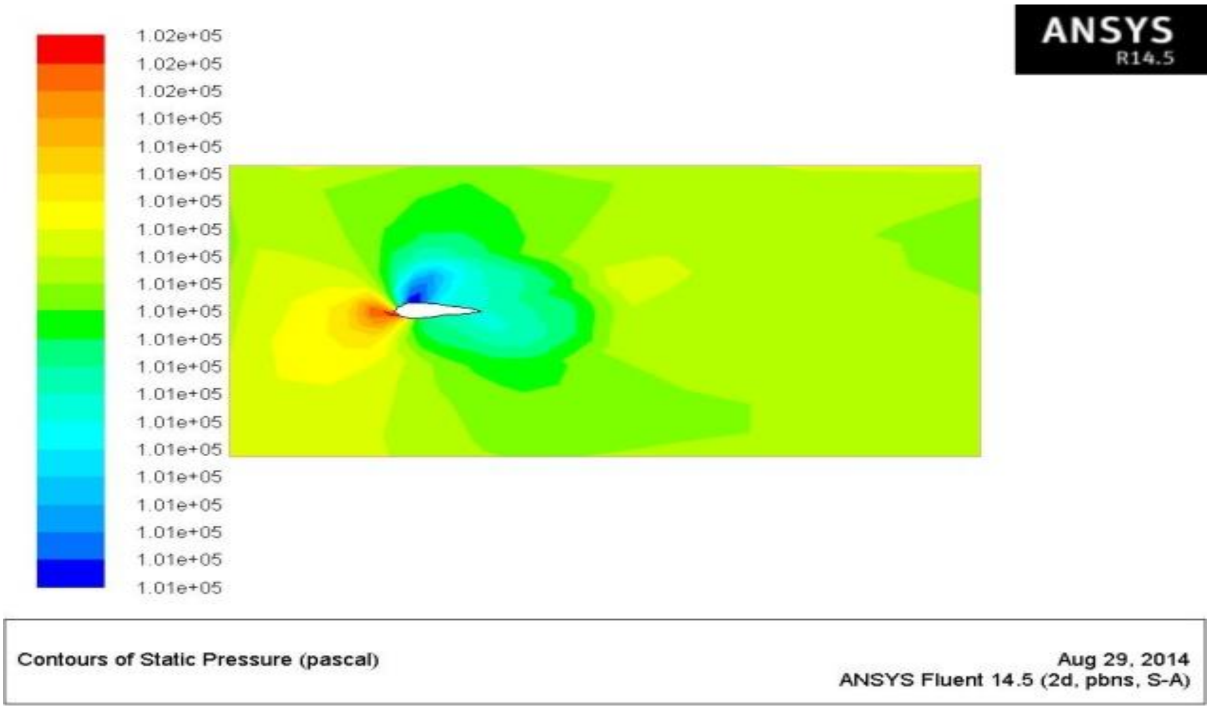

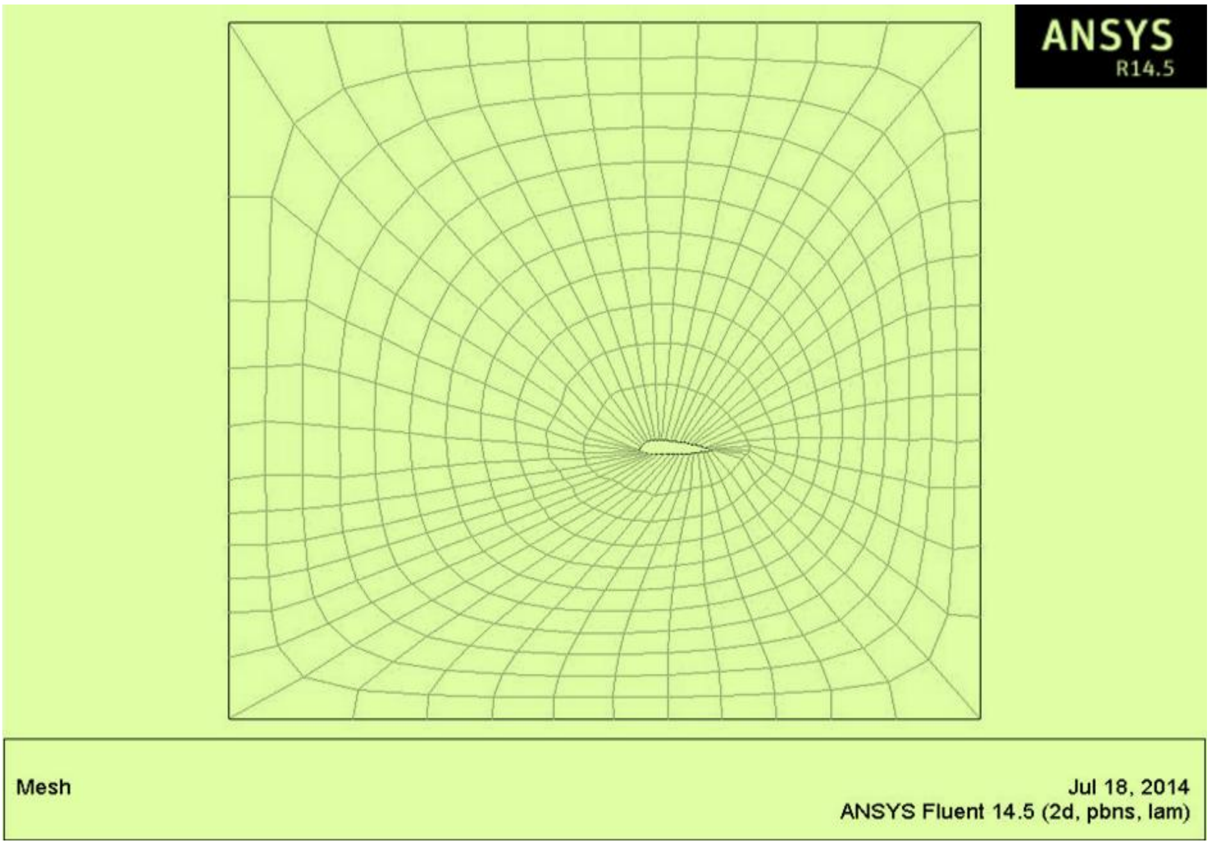

Figure-12: Meshing geometry of the Rear rotor

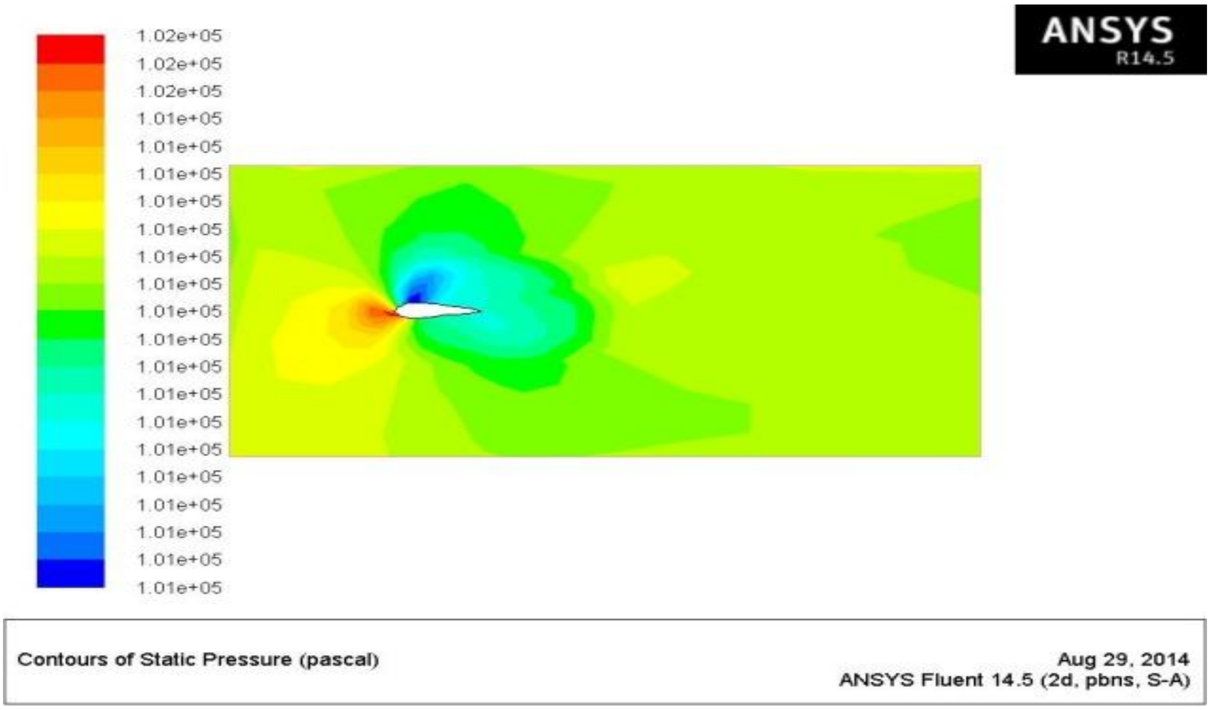

Figure-13: Pressure Contour at AOA 10° for Front Rotor

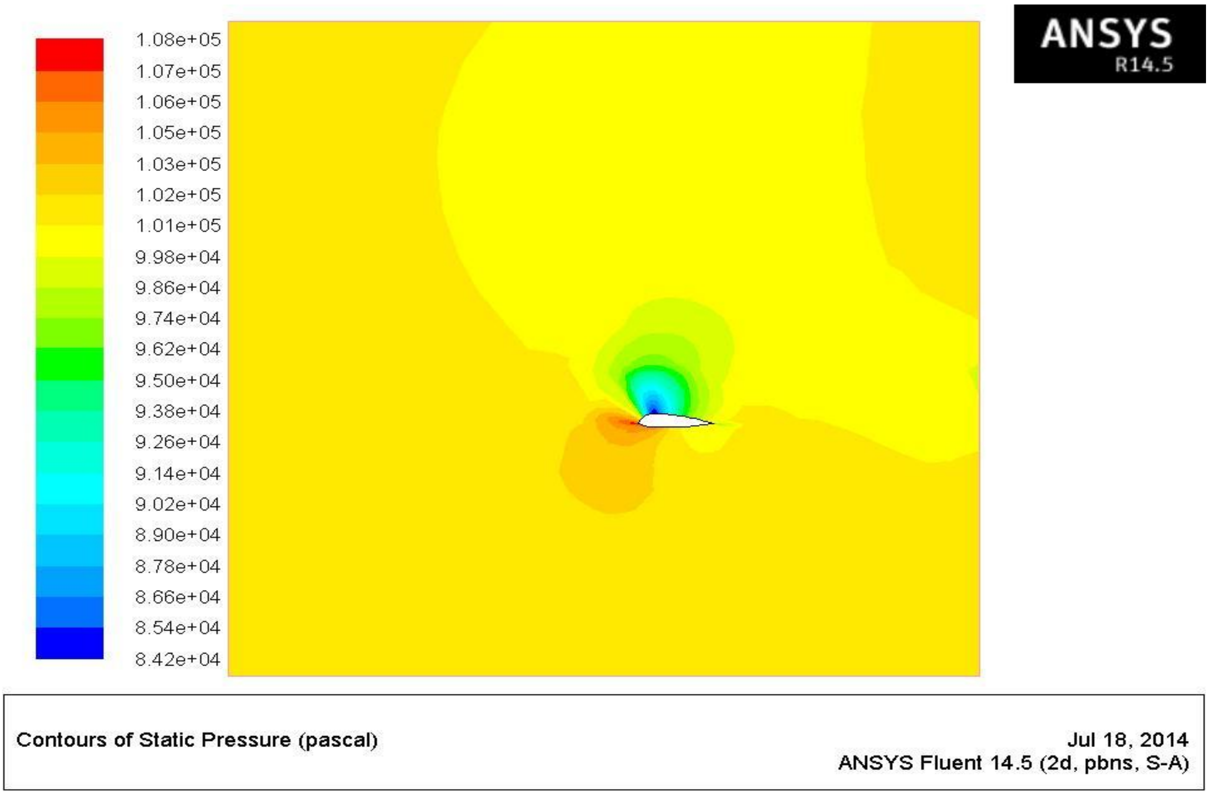

Figure-14: Pressure Contour at AOA 10° for Rear Rotor

12. MATERIAL SELECTION FOR GEARBOX SYSTEM

The material used for the manufacture of gears depends upon the strength and service conditions like wear, noise etc. The gears may be manufactured from metallic or non-metallic materials. The metallic gears with cut teeth are commercially obtainable in cast iron, steel and bronze. The non-metallic materials like wood, rawhide, compressed paper and synthetic resins like nylon are used for gears, especially for reducing noise. The cast iron is widely used for the manufacture of gears due to its good wearing properties, excellent machinability and ease of producing complicated shapes by casting method. The cast iron gears with cut teeth may be employed, where smooth action is not important. The steel is used for high strength gears and steel may be plain carbon steel or alloy steel. The steel gears are usually heat treated in order to combine properly the toughness and tooth hardness. [14]

13. DESIGN METHODOLOGY OF GEAR MECHANISM

The Designing of gearbox is done on the powerful CAD software CATIA.
For designing a gearbox first we have to determine its design considerations which are as follows:-

In the design of a gear drive, the following data is usually given [14]:
1. The power to be transmitted.
2. The speed of the driving gear,
3. The speed of the driven gear or the velocity ratio

Total Power of the wind on our front blades of Dual Rotor wind turbine system:-

$$P= \frac{1}{2}\rho AV^3 \qquad (1)$$

Where ρ is density of air taken $1.25 kg/m^3$
V is Rated wind velocity taken 10m/s
and A is Swept are of wind turbine rotors.

In this wind turbine we had taken the blade length of 1.5m
Hence the swept area of the wind turbine rotor is

$$A=\pi R^2$$

On putting all these values in equation 1 we will get Total Wind power is

$$P=\frac{1}{2}*1.2\times\pi\times1.5^2\times10^3$$

$$P=4309.65W$$

Similarly we will calculate wind power in rear rotor also; however the wind speed on the rear rotor decreases due to obstruction of front wind blades. It has been found that maximum wind speed at the front rotor is 2/3rd of the free stream hence only 1/3rd of the wind speed will reach at the rear rotor. This 1/3rd velocity of the wind will hit the shadow area of Rear rotor, Since our rear rotor is 3 times radius than front rotor, The Front rotor is in shadow area hence the velocity of wind at rear rotor will be almost same,

$$V_{REAR}\approx V_{FRONT}$$

Torque available at the gear,

$$T = \frac{P*60}{2\ \pi N} \qquad (2)$$

For our wind turbine system,

Assuming tip speed ratio (λ) =3

λ = speed of rotor/speed of wind

$$V=\omega.R. \qquad (3)$$

$$V= (2\times\pi\times N\times R)/60$$

$$V= (2\times3.14\times N\times1.5)/60$$

$$10*60 = 9.42N$$

$$N=63.69\approx65rpm$$

This is rotational wind speed,
Rotor speed will be,

$$\text{Tip speed ratio } (\lambda) = \frac{\text{speed of rotor}}{\text{speed of wind}} \qquad (4)$$

$$\lambda =3$$

$$\frac{\text{speed of rotor}}{65}=3$$

$$N=195\ RPM$$

Hence torque will be,

$$T= (4309.65*60)/ (2*\pi*195)$$

$$T=211.15 N\text{-}m$$

By the help of torque, power and gear ratio and by using the following formulae's we can determine the design values of different gears, shafts and keys of our gearbox.

13.1 Designing of Gears

In this gearbox design the assembly of sun and planet gears is bit different from other epicyclic train. The power from wind energy which is converted to rotational energy by rotor blades is transferred to the transmission system or its called gearbox system. The input wind energy from both front and rear side rotor in the form of torque transferred into the sun gear, the sun gears are in the direct mesh with planet gears. The torque from both sun gears is then transferred to crown wheel. The crown wheel is in direct mesh with output pinion gear. We had taken the gear ratio of crown wheel and output pinion gear as 1:4. From output pinion gear it goes to input spur gear.

13.2 Designing of the Sun, Planet, and Bevel Gears.

For designing any gear drive, first we have to assume the gear ratio. Let the gear ratio be G.
Minimum number of teeth to avoid interference

$$T_P=\frac{2A_W}{G[\sqrt{1+\frac{1}{G}\left(2+\frac{1}{G}\right)\sin^2\delta}-1]} \quad (5)$$

T_P=Number of teeth on pinion
A_w = Fraction by which the standard addendum for the wheel should be multiplied,
G= Gear ratio of pinion and gear,
δ = Pressure angle of the gear, we will take pressure angle 20° full depth involute system.
This will give us minimum number of teeth on pinion, and by using gear ratio problem we can calculate number of teeth on gear drive also as follows:-

$$\frac{T_G}{T_P} = G \quad (6)$$

Now we determine the pitch angle (Θ_{p1}) for the pinion and gear (Θ_{p2})

$$\Theta_{p1}= \tan^{-1}\left(\frac{1}{v.r}\right) \quad (7)$$

And,

$$\Theta_{p2}= (90- \Theta_{p1}) \quad (8)$$

Where,
Θ_{p1}=pitch angle of Gear
Θ_{p2}=pitch angle of pinion

The Tangential load on the pinion is to be calculated, so that we can apply Lewis equation to determine the module.
Hence Tangential load on pinion is given by,

$$F_T = 2T/D_p$$

Where T= Torque and D_P= pitch circle diameter of the pinion

We Knows that,

$$D_P =m.T_p \quad (10)$$

Here m is module of the gears.

The Length of the pitch cone element (L) of a bevel gear is calculated as follows,

$$L=\frac{D_P}{2\sin\theta_{P_1}} \quad (11)$$

The face width for the gear can be assumed between L/3 to L/4
In this gear we has assumed the face width (b)

$$b=L/3$$

Putting all these values in Lewis equation as follows,

$$F_T = (\sigma_{op} \times C_V)\, b \times \pi \times m \times y_P \times \frac{(L-b)}{L} \quad (12)$$

Where,
σ_{op}=Allowable static stress of pinion
C_V=Velocity factor
b=face width
y_P=Tooth form factor or Lewis factor

We will get the cubic equation in the form of m and by solving this equation we will get value of 'm'.
The value of 'm' is used to calculate other dimensions of a gear. We had used above given formulae's to design the bevel gears, sun gear, planet gear, crown wheel and output pinion gear.

The Torque from output pinion gear is transmitted to input spur gear. The value of torque is calculated as follows.

$$\frac{\text{Torque on output pinion gear}(T)_1}{\text{Torque on input spur gear}(T)_2} = G \quad (13)$$

We know the values of torque on Output pinion gear; we can calculate torque on input spur gear by the help of gear ratio (G).
After finding the torque we will apply the same procedure on spur gear calculation as in the case of bevel gear and find the dimensions of spur gears.

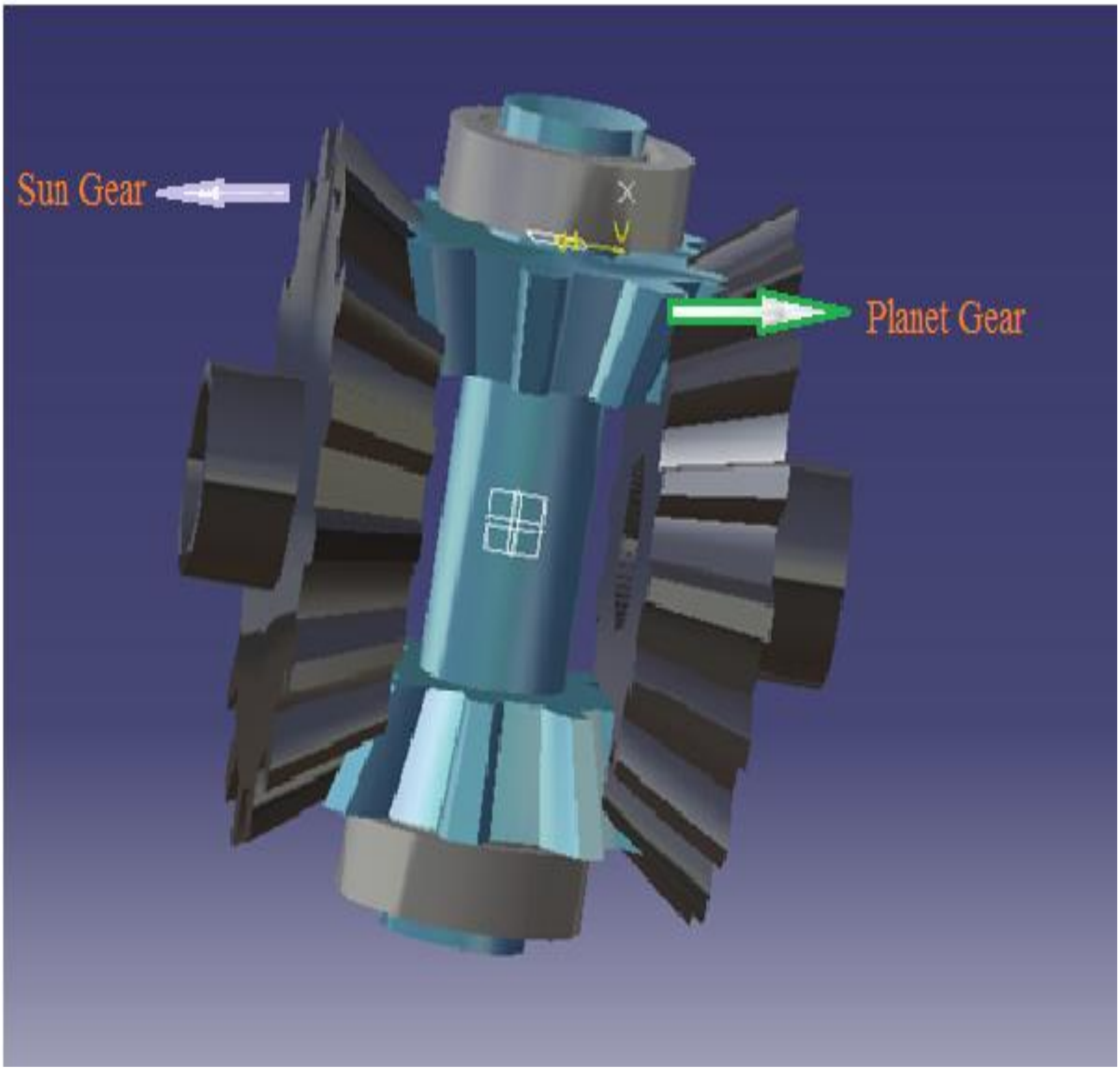

Figure -15:- Sun& Planet Gears Designed On Catia

Table -4:- Design Perimeters for Sun And Planet Gears

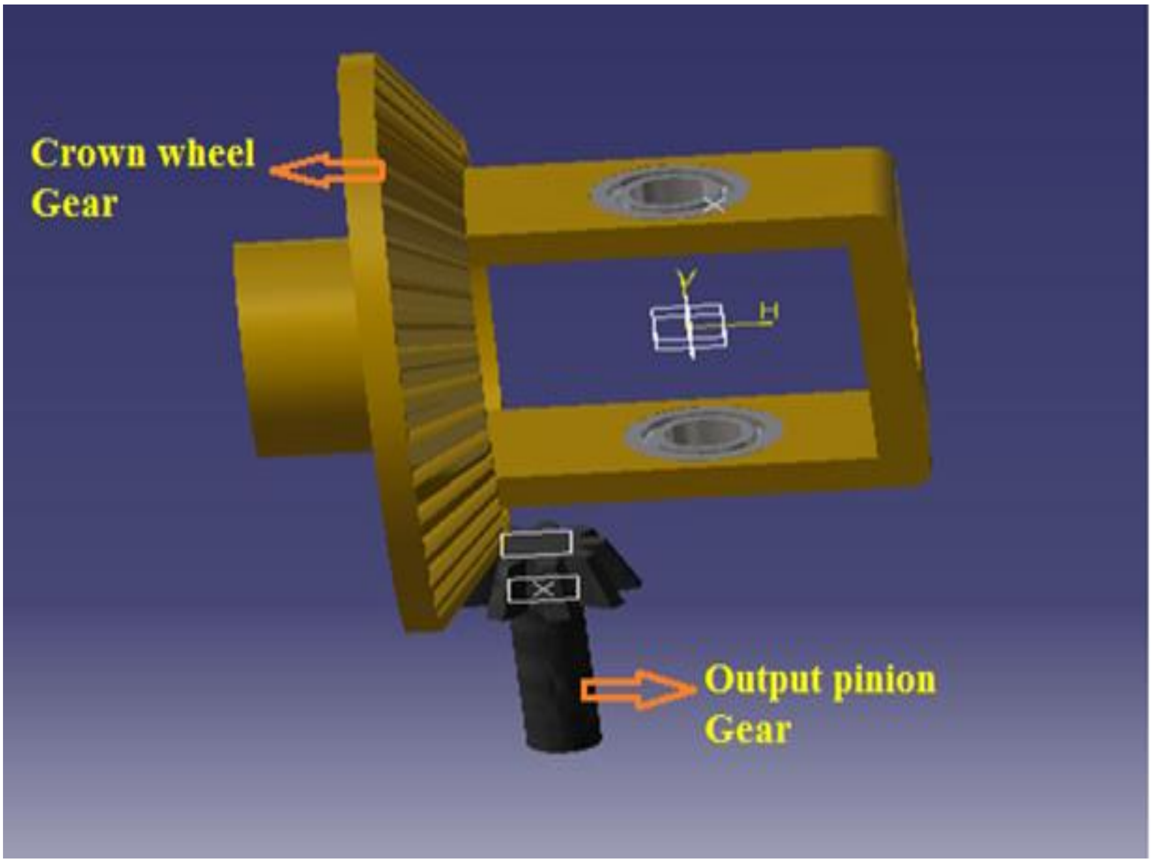

Figure- 16:-Catia Design of Crown Wheel And Output Pinion Gear

Table -5:- Design Perimeters for Crown Wheel And Pinion

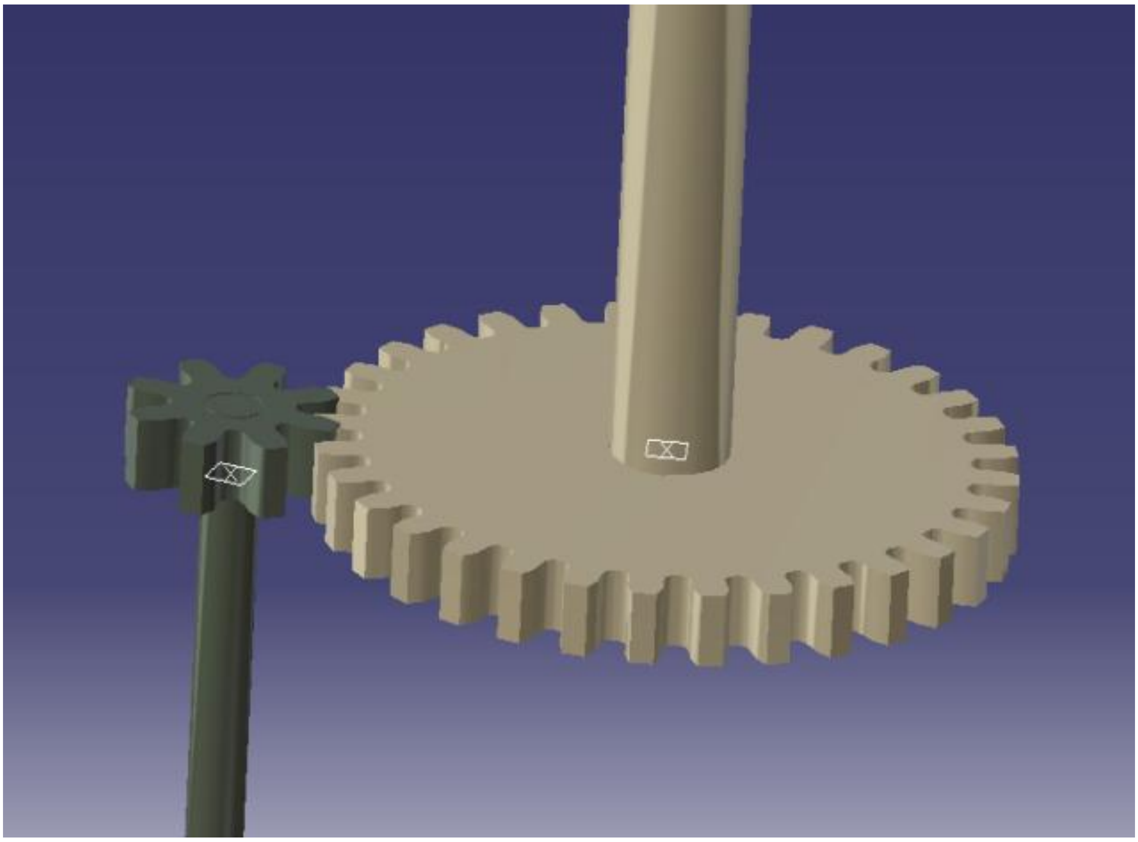

Figure -17:-Design of Spur Gear

Table- 6:-Spur Gear Dimensions

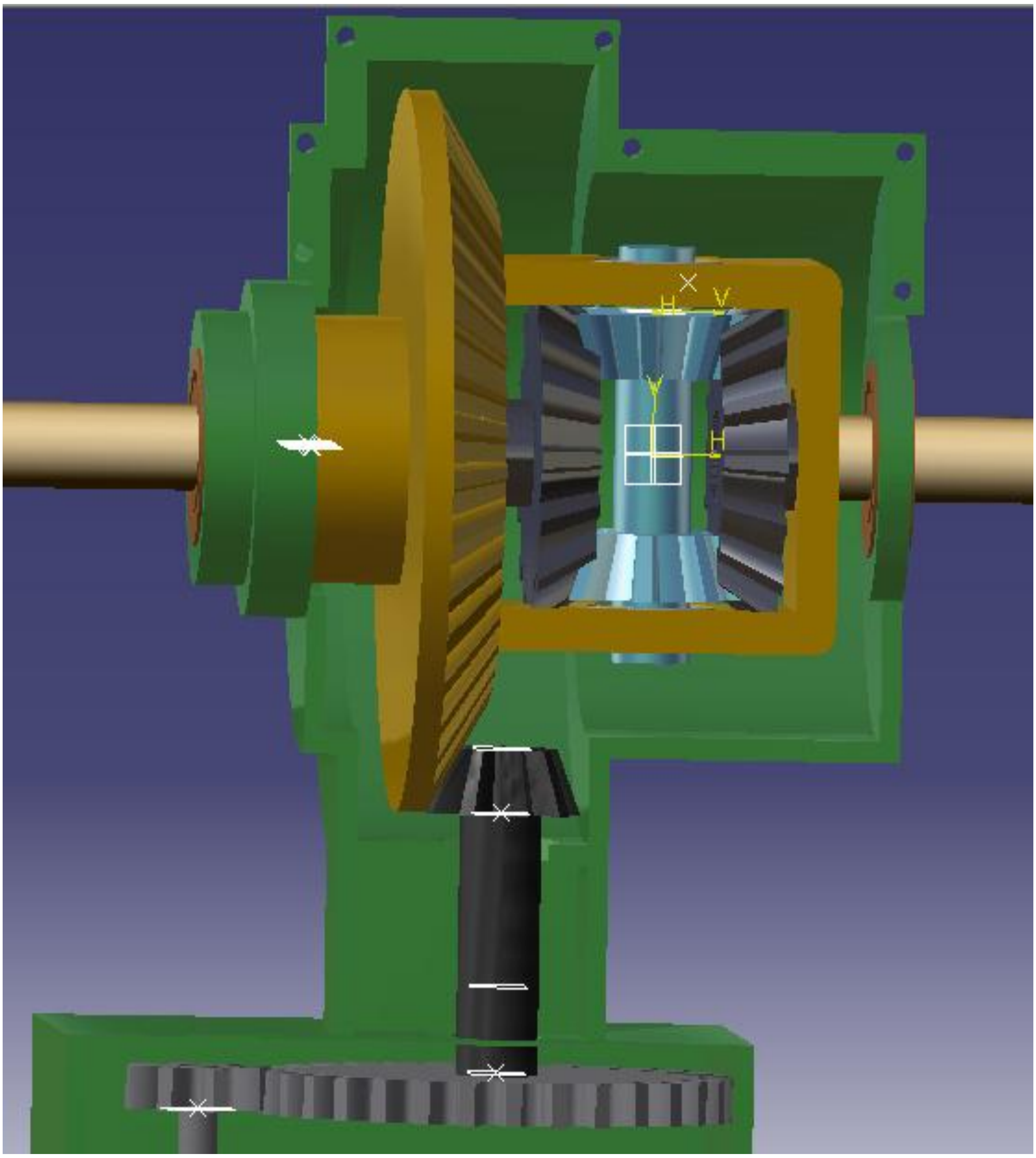

Figure 18. The Proposed Gearbox Of Dual Rotor Wind Energy System

14. DESIGNING OF GEAR SHAFTS AND KEY SPLINES.

A shaft is a rotating machine element which is used to transmit power from one place to another. The power is delivered to the shaft by some tangential force and the resultant torque (or twisting moment) set up within the shaft permits the power to be transferred to various machines linked up to the shaft. In order to transfer the power from one shaft to another, the various members such as pulleys, gears etc., are mounted on it. These members along with the forces exerted upon them causes the shaft to bending. In other words, we may say that a shaft is used for the transmission of torque and bending moment. [14]

The shafts may be designed on the basis of
1. Strength, and
2. Stiffness & Rigidity

In designing shafts on the basis of strength, the following cases may be considered:
(a) Shafts subjected to twisting moment or torque only,

(b) Shafts subjected to bending moment only,
(c) Shafts subjected to combined twisting and bending moments, and
(d) Shafts subjected to axial loads in addition to combined torsional and bending loads.

In order to find the diameter of shaft for gears, the following procedure may be followed:-

1. First of all, find the normal load (F_N), acting between the tooth surfaces. It is given by

$$F_N = F_T / \cos\delta \qquad (14)$$

2. The weight of the gear is given is calculated by

$$F_G = 0.00118 * T_G * b * m^2 \text{ (in N)} \qquad (15)$$

3. Now the resultant load acting on the gear is calculated

$$F_R = \sqrt{F_N^2 + F_G^2 + 2F_N F_G \cos\delta} \qquad (16)$$

4. If the gear is overhung on the shaft, then bending moment on the shaft due to the resultant load,

$$M = F_R \times X \qquad (17)$$

Where X = Overhang i.e. the distance between the centre of gear and the centre of bearing.

5. Since the shaft is under the combined effect of torsion and bending, therefore we shall determine the equivalent torque. We know that equivalent torque,

$$T_E = \sqrt{(M)^2 + (T)^2} \qquad (18)$$

6. Now the diameter of the gear shaft (d) is determined by using the following relation,
We also know that equivalent twisting moment (T_E)

$$T_E = (\pi/16) \times \tau \times d^3 \qquad (17)$$

τ =Shear stress of the shaft
We have used above Equations to calculate the diameter of Gear Shafts.

15. BEARING DESIGN FOR GEARBOX

A bearing is a machine element which supports another moving machine element (known as journal). It permits a relative motion between the contact surfaces of the members, while carrying the load. Bearings in wind turbines operate at the extremes of operational environments in terms of temperature, load fluctuation, maintenance access and lubricant optimization. As rotor diameters increase, confidence in your bearings becomes even more critical.

Generally For wind turbine Gearbox spherical roller bearing for large wind turbine are used but for small gearboxes Ball bearing is used. We are using radial ball bearings for our Gearbox. In this Gearbox we have designed a radial ball bearing.

For Designing the Bearing we need basic dynamic load rating(C) & Diameter of Shaft.
Basic dynamic load rating(C)

$$C = W \times \left(\frac{L}{10^6}\right)^{1/6} \qquad (18)$$

L=Life of bearing, in hours, Assuming of bearing life of wind turbine gearbox 100000 Hours.

Where W is the dynamic equivalent radial load, which is determined by radial load (FR) and constant axial or thrust load (FA)

$$W = X.\ V.\ F_R + Y.\ F_A \qquad (19)$$

Where V = A rotation factor,

F_R = Radial load,

F_A = Axial or thrust load,
X=radial load factor

Radial Load (F_A) and Axial Load (F_R) is Determined by following Formulae

$$F_A = F_T \tan\alpha \sin\delta \tag{20}$$

$$F_R = F_T \tan\alpha \cos\delta \tag{21}$$

α =Nominal angle of contact
δ= Pressure angle of gear
By putting all values in equation (18) we get dynamic load rating.
Hence we get the value of C and for the diameter of shaft of diameter 'd' we can use standard value of Ball Bearing no. 6407 from PSG Design Data book.

16. RESULTS AND CONCLUSION

A review and research study of a horizontal axis wind turbine blade design and Gearbox has been carried out with an existing generator and a wind speed resource on Design softwares like ANSYS & CATIA.In this Research paper we have studied the designing of the Gearbox of dual rotor wind turbine system. CATIA software for the designing of the gearbox. But calculation for the dimensions of gear is done by basic formulae's. Basic formulae's for calculating gear dimensions are discussed and tables of gear dimensions are drawn in this paper. This gearbox has two input shafts and one output shaft. The dual rotors in front and rear side capture wind energy. The captured wind energy is transformed into high speed rotational energy by transmission system. In case of single rotor only single front rotor can convert wind energy into useful energy but in this research paper had designed a dual rotor wind turbine gearbox on CATIA which can generate about 5% more power than conventional wind turbine system.
CFD is widely used for analysisof flowpattern around the wind turbine rotor (e.g. velocity and pressure distribution) which is affected by wind velocity, angle of attack, tip speed ratio etc. With a rated wind speed of 10m/s and a generator of 1.5kW. A further structure analysis and testing will be developed in the future.The table-6 shows the various forces acting on blades.

Table -7: Force Calculation on the ANSYS FLUENT software.

To study the effects of roughness on the wind flow, the roughness of the whole area surrounding the site was put into consideration and the area was divided into various roughness classes and as a result it was observed that roughness is a crucial factor in predicting the wind flow. In order to study the prevailing wind climate at the site, wind data was recorded at Energy park wind mast of Location East 077' 21.668 and North 23' 18.720 for the duration of One year from 04 July 2016 to 4 July 2017. It was observed from the wind roses that wind flows predominantly in 10 and 11 sectors from the West-North, West(270°-300°) taking North as reference at 0° indicating a strong influence of the rainy season in the Indian subcontinent. It was found out that mean wind speed and mean power density at 20 meter height was 3m/s and 23 W/m^2 respectively, with minimum and maximum wind speed 0.40 m/s and 16 m/s respectively.

Recent progresses in wind turbine aerodynamics have been selectively presented in this paper. BEM theory, regardless of its simplification, is still a daily design tool for wind turbines. However, BEM method has many natural shortcomings, and relatively less ability to model the physics of the turbine aero dynamics in the field of high unsteadies conditions, such as atmospheric turbulence, wind shear, deep stall, in tractions of neighbouring turbines, wake and etc. Therefore, more sophisticated vortex wake models have been developed to directly deal with vortices that dominate the wind turbine flow field in essence and therefore may provide relatively reliable information although they require more validations. Introduction of dynamic stall model and 3D rotational effect model greatly improves the wind turbine aerodynamic load calculations. However, more accurate dynamic stall models and delay stall models are required, which can be developed only through much more experimental and computational studies. CFD methods have provided deep insight to wind turbine flow fields. However, CFD methods have not been used for design purposes with confidence.

REFRENCES

1. Acker, T. and Chime, A.H., 2011, "Comparison of the actual and predicted wind energy production of a wind turbine using windpro and WAsP software"

2. B. G. Newman, Actuator-disc theory for vertical-axis wind turbines. Journal of Wind Engineering and Industrial Aerodynamics, 15, 1983, pp.347-355.

3. Carlo Ennico carangid, 2008, 'Wind turbine functioning and aerodynamics', CFD-RANS study of Horizontal Axis Wind Turbine, Italy.

4. Craig, K.J., Venter, P.J., de Kock, D.J., Snyman, J.A., "Optimisation of structured grid spacing parameters for separated flow simulation using mathematical optimisation," J. Wind Engg. Ind. Aerodynes. 80 (1999) pp. 221-231.

5. Drela, M., “XFOIL: An Analysis and Design System for Low Reynolds Number Airfoils,” MIT Dept. Of ronautics and Astronautics, Lecture Notes in Engineering, No. 54, 1989, pp.1-12.

6. Du, Z., Selig, M.S. “The Effect of Rotation on the Boundary Layer of a Wind Turbine Blade,” Renewable Energy 20 (2000) pp. 167 – 181.

7. Fluent Inc, “Transport Equation for the Spalart-Allamras Models Theory” FLUENT 6.3 User’s Guide FLUENT Inc.

8. Hau Erich. Wind turbines: fundamentals, technologies, application, economics. New York: Springer; 2000. pp.67-80.

9. J.D. Booker, P.H. Mellor , R. Wrobel & D. Drury, “A compact, high efficiency contra-rotating generator suitable for wind turbines” Elsevier journal of Renewable Energy 35 (2010) ; 2027-2033.

10. Karl, J.N., 2010, “Estimation of wind energy production in relation to orographic complexity”.

11. Mortensen, N.G. Heathfield, D.N. Rathmann, O. and Morten, N., 2013, “Wind Atlas Analysis and Application Program: WAsP 11 Help Facility.

12.Sveinbjornsson, S., 2013, “Analysis of WAsP (Wind Atlas Analysis and Application Program) in Complex topographical Conditions using measured production from a large scale wind farm

13.Shen, W.Z. Zakkam, V.A.K. Sorensen, J.N. and Appa K. “Analysis of Counter-Rotating Wind Turbines”. Lyngby, Denmark: Technical University of Denmark. 2007.

14. R.S Kurmi(2005) J.K Gupta, A Textbook Of Machine Design By R.S Kurmi(2005) J.K Gupta Eurasia Publishing House Printed Edition.

15. “Design Data Book” 2011 PSG College of Technology.

